ELSEVIER International Journal of Mass Spectrometry 210/211 (2001) 459–468 www.elsevier.com/locate/ijms

A mechanistic investigation of the reactions between the *tert*-butyl methylene oxonium ion [$CH_2OC(CH_3)_3^+$] and ammonia: competition between substitution, addition-elimination, and elimination

Lihn Bache-Andreassen, Einar Uggerud

Department of Chemistry, University of Oslo, P.O. Box 1033 Blindern, N-0315 Oslo, Norway

Received 3 January 2001; accepted 14 February 2001

Abstract

Fourier transform ion cyclotron resonance mass spectrometry and ab initio calculations have been used to investigate the reactions between $CH_2O(CH_3)_3^+$ (**1**) and NH_3 (**2**). The main primary reactions are formation of $CH_2O\cdots H{-}NH_3^+$ (**14**) and NH_4^+ (**15**). In addition to this, small and approximately equal amounts of $CH_2NH_2^+$ (**17**) and $(CH_3)_3CNH_3^+$ (**5**) are formed. Rice–Ramsperger–Kassel–Marcus (RRKM) reaction rate calculations confirm that in spite of the substantial difference in the energy of the transition structures for $CH_2NH_2^+$ and $(CH_3)_3CNH_3^+$ formation, the rate constants for these two reactions approach each other at thermal energies for the reactants. The proton bonded dimer between ammonia and formaldehyde formed upon *i*-butene loss undergoes a ligand-exchange reaction with ammonia forming $(NH_3)_2H^+$ (**9**). The MP2/6-31G(d,p) calculations predict that all the reactions are exothermic with transition states below the energy of the reactants, except for the formation of the ammonium ion which is calculated to be slightly endothermic. The results of the more accurate G2-method calculations indicate that the latter process probably is slightly exothermic - in accordance with the experiments. (Int J Mass Spectrom 210/211 (2001) 459–468) © 2001 Elsevier Science B.V.

Keywords: Mass spectrometry; Quantum chemistry; Reaction mechanism

1. Introduction

Oxonium ions are known to be ambidente, having two electrophilic centers; one at the carbonyl carbon and one at the α-carbon of the oxygen substituent. We have previously investigated the reactions between CH_2OR^+ ions [R=H, CH_3, CH_2CH_3, $CH_2CH_2CH_3$, $CH(CH_3)_2$] and ammonia, both through theoretical calculations and experiments [1]. All these oxonium ions showed the anticipated behavior with reactions resulting from attack of ammonia at both electrophilic centers, respectively. Attack at the carbonyl carbon initiates an addition-elimination (**ae**) reaction, with elimination of an alcohol. A backside attack at the oxygen substituent leads to a nucleophilic substitution (**sub**) reaction with formaldehyde as the leaving group.

---

* Corresponding author. E-mail: einar.uggerud@kjemi.uio.no

Dedicated to Professor Nico M. M. Nibbering for his commitment and contributions to mass spectrometry and ion chemistry.

PII S1387-3806(01)00437-7

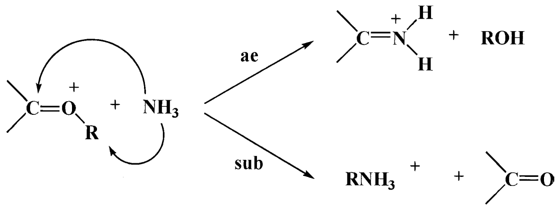

Scheme 1.

This dualistic behavior have also been observed by others in reactions between oxonium ions and ammonia, alcohols, ethers, aldehydes, ketons, and other classes of organic compounds [2–10]. In principle, elimination (**e**) may compete with substitution. This was inferred by us from quantum chemical calculations showing that formaldehyde either may be lost in a normal S_N2 fashion (**sub**) or via an elimination route (**e**) [1] in the reactions

$$CH_2OCH(CH_3)_2^+ + NH_3 \rightarrow$$

$$(CH_3)_2CHNH_3^+ + CH_2O \qquad (1)$$

$$CH_2OCH(CH_3)_2^+ + NH_3 \rightarrow$$

$$CH_3CHNH_2\cdot\cdot\cdot H-NH_3^+ + CH_2O \qquad (2)$$

Other examples on the competition between S_N2 and E2 in the gas phase have also been reported [11–14].

The tertiary butyl group is a particularly interesting substituent, both because of its high intrinsic stability and its bulkiness. We would therefore expect the *t*-butyl cation to be less strongly bonded to formaldehyde than the smaller alkyl groups. For this reason it is likely that it has a higher ability to build ion-neutral complexes (INC) [15,16], which also increases the possibility of flat plateaus on the potential energy surfaces. Norrman and McMahon [17] have studied the structures of complexes between $(CH_3)_3C^+$ and small organic molecules, and they found that adducts may exist in two isomeric forms; one covalent bonded isomer that dominates at low temperatures and one electrostatic bonded that dominates at high temperatures.

In this paper we will focus on the reactions between ammonia and the *t*-butyl methylene oxonium ion, $CH_2OC(CH_3)_3^+$. The purpose of this is twofold. Firstly, we are interested to learn which role ion neutral complexes play. Secondly, this study completes the previous one, making it possible to systemize the observations in terms of substituent effects.

2. Experimental and theoretical methods

2.1. Mass spectrometric experiments

All experiments were conducted with a Fourier transform ion cyclotron resonance mass spectrometer (Apex 47e, Bruker Daltonics, Billerica, MA, USA) equipped with an external ion source. The $CH_2OC(CH_3)_3^+$ ions were formed by 25–35 eV electron impact on *t*-butyl *n*-propyl ether in the external on source. The mixture of ions made in this process was transferred to the ICR cell, which contained NH_3 at a stationary partial pressure of typically 5×10^{-9} mbar. All ions except the wanted $CH_2OC(CH_3)_3^+$ ions were ejected from the cell by correlated frequency sweep[18]. To get rid of excess energy by collisional deactivation, argon was introduced into the cell via a pulsed valve (peak pressure 10^{-5} mbar) and then allowed to pump away for 3–4 s. This thermalized population of the $CH_2OC(CH_3)_3^+$ ions were then again isolated, this time by single frequency shots to eject fragments and reaction products formed during the cooling period. The mass spectrum was then recorded after a variable reaction time to investigate the time development of the reactions between $CH_2OC(CH_3)_3^+$ and NH_3. To get a clearer picture of the reaction sequences, several of the products were isolated with correlated frequency sweep and allowed to react further with ammonia.

The *t*-butyl *n*-propyl ether used in the mass spectrometric experiments was prepared according to a literature procedure [19].

The small amount of $CH_2OC(CH_3)_3^+$ present in the cell after the final isolation procedure has hampered our investigation. There are two reasons. Firstly, the amount of $CH_2OC(CH_3)_3^+$ resulting from ethyl radical loss from $CH_3CH_2CH_2OC(CH_3)_3^{+\cdot}$ is very small (1%) compared to the more energetically favorable $CH_3CH_2CH_2OC(CH_3)_2^+$ fragment. Secondly, the rather weak bond between CH_2O and $C(CH_3)_3^+$ may break during the collisional cooling event. The combined result of these factors is that the signal-to-noise (S/N) ratio was quite poor. In an attempt to improve the yield of $CH_2OC(CH_3)_3^+$ we tried to make the ions by association between CH_2O and $C(CH_3)_3^+$ in the external ion source (*i*-butane chemical ionization of CH_2O), but this was not successful.

The measurements were repeated in several different sessions to ensure long time reproducibility, and the instrument was operated at sufficient high resolution to identify reactants and products by precise mass measurement.

2.2. Quantum chemical model calculations

Quantum chemical calculations were carried out using the program systems GAUSSIAN 94 [20] and GAUSSIAN 98 [21]. The quantum chemical methods used were Hartree–Fock (HF) [22] and Møller–Plesset perturbation theory to the second order (MP2) [23] with 3-21G and 6-31G(d,p) basis sets [24]. Where possible, all relevant critical points (reactants, transition structures, intermediates, and products) of the potential energy surface were characterized by complete optimization of the molecular geometries for HF/3-21G and MP2/6-31G(d,p). Relative energies were calculated by including the zero-point vibrational energies (zpve) scaled by a factor of 0.9207 for the HF/3-21G and 0.9608 for the MP2/6-31G(d,p) calculations [25].

2.3. Rice–Ramsberger–Kassel–Marcus reaction rate calculations [26]

A standard computer procedure was employed to calculate theoretical rate coefficients for some of the reactions. The normal vibrational frequencies from either the HF/3-21G or MP2/6-31G(d,p) calculations were used as input. Details of the calculations (list of frequencies, etc.) may be obtained from the authors upon request.

3. Results

Two mass spectra from the reaction between $CH_2OC(CH_3)_3^+$ and ammonia taken after short and long reaction times, respectively, are shown in Fig. 1. From the spectra it is evident that the primary reaction products are at *m/z* 18, 30, 48, and 74, and that that the major final products are at *m/z* 18 and 35. The proposed reaction scheme is shown in Scheme 2 and will be explained below. The geometries of the

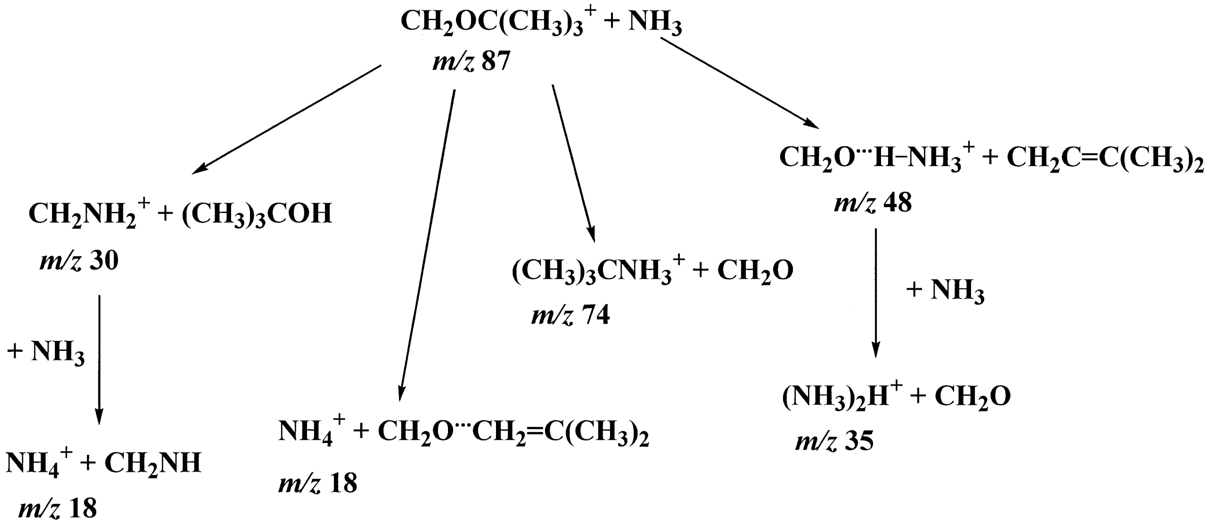

Scheme 2.

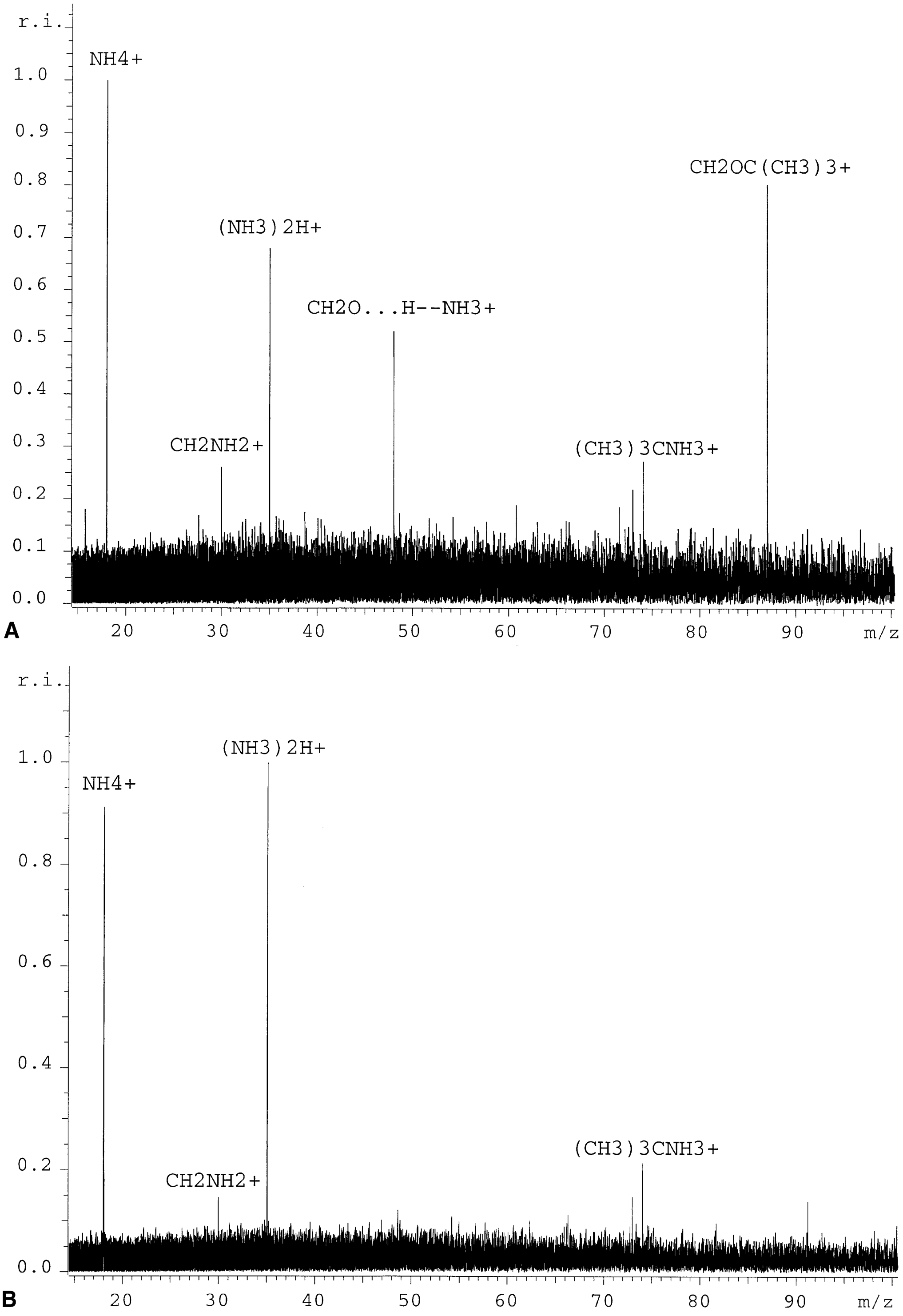

Fig. 1. Mass spectra of the reaction between (a) $CH_2OC(CH_3)_3^+$ and (b) NH_3 recorded at a nominal pressure of $P(NH_3) = 8.8 \times 10^{-09}$ mbar. The uppermost spectrum was recorded after a reaction time of 4 s, and the spectrum at the bottom after 20 s.

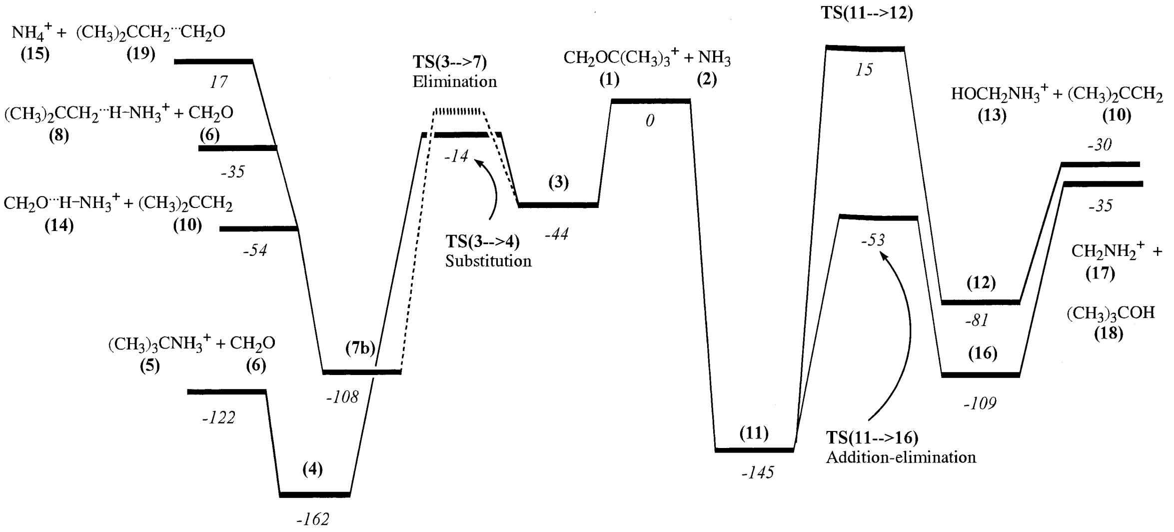

Fig. 2. Structures of the stationary points obtained with MP2/6-31G(d,p). Bond lengths are given in A°.

optimised structures are shown in Figure 3 and the corresponding absolute energies in Table 1.
The geometries of the optimized structures are shown in Fig. 2 and the corresponding absolute energies in Table 1.

3.1. The formation and reactions of $(C_4,N,H_{12})^+$-ions (m/z 74.095)

The ab initio calculations show that three different exothermic reaction channels lead to ions of this elemental composition. The NH_3 (**2**) molecule may attack the central carbon of the *t*-butyl substituent from the face opposite to that of the leaving group, CH_2O (**6**), and the transition structure for this S_N2 mechanism, **ts(3 → 4)** lies 14 kJ/mol lower in energy than the reactants (Fig. 3). The products of this reaction are formaldehyde (**6**) and protonated *t*-butyl amine (**5**) and the reaction is exothermic by 122 kJ/mol. There seems to be a second transition state in this mechanism, where one of the methyl groups in the *t*-butyl part rotates to permit for a shorter distance between the central carbon atom and ammonia. This transition state is expected to be lower in energy, so we did not try to localize it. The ammonia molecule may also attack the O-substituent from the same side as the leaving group, in a front-side nucleophilic substitution reaction. We did not perform this calculation due to the extreme computer resources that these calculations require. On the basis of what we know about a closely related reaction [13], it is reasonable to assume that front-side substitution is feasible, probably with a barrier approximately 10 kJ/mol above **ts(3 → 4)**. The third route that may lead to an ion of this elemental composition is an elimination reaction (**e**). This mechanism starts with the formation of the same hydrogen bonded INC between the reactants (**3**) as the back-side substitution mechanism, followed by a proton transfer from the *t*-butyl part to ammonia (**ts(3 → 7)**). Unfortunately, we have not been able to localize a transition structure with MP2/6-31G(d,p), only with HF/3-21G. The HF/3-21G barrier was calculated to be 23 kJ/mol lower in energy than the reactants. This leads to a second INC (**7a**) where CH_2O and NH_4^+ are hydrogen bonded to *i*-butene. As mentioned in the introduction, we found a similar mechanism in the reaction between $CH_2OCH(CH_3)_2^+$ and NH_3, but in that case it was shown that when the proton is transferred to NH_3, CH_2O detaches and moves around the remaining C_3H_6 unit to form a proton bonded trimer between ammonia, formaldehyde, and propene. Formaldehyde was then eventually expelled with a hydrogen-bonded heterodimer between ammonium and propene as the

Table 1
Absolute energies of the optimized structures shown in Fig. 3; Zpve scaled by 0.9207 (HF/3-21G) and 0.9608 [MP2/6-31G(d,p)] are included

Molecule	HF/3-21G (Hartree)	MP2/6-31G(d,p) (Hartree)
$CH_2OC(CH_3)_3^+$ **(1)**	−268.69238	−271.08853
NH_3 **(2)**	−55.83903	−56.34913
$CH_2OC(CH_3)_3 \cdots NH_3^+$ **(3)**	−324.54969	−327.45461
ts(3→4)	−324.54013	−327.44310
$CH_2O \cdots C(CH_3)_3NH_3^+$ **(4)**	−324.59530	−327.49918
$(CH_3)_3CNH_3^+$ **(5)**	−211.38054	−213.32680
CH_2O **(6)**	−113.19514	−114.15718
ts(3→7)	−324.54013	· · ·
$CH_2O \cdots (CH_3)_2CCH_2 \cdots NH_4^+$ **(7a)**	−324.55584	−327.46160
$(CH_3)_2CCH_2 \cdots NH_4^+ \cdots CH_2O$ **(7b)**	−324.57903	−327.47865
$(CH_3)_2CCH_2 \cdots H\text{-}NH_3^+$ **(8)**	−211.34744	−213.29382
$NH_3 \cdots H \cdots NH_3^+$ **(9)**	−112.08065	−113.08168
$(CH_3)_2CCH_2$ **(10)**	−155.14035	−156.58528
$NH_3 \cdots CH_2OC(CH_3)_3^+$ **(11)**	−324.59396	−327.49286
ts(11→12)	−324.52384	−327.43192
$NH_3CH_2OH \cdots CH_2C(CH_3)_2^+$ **(12)**	−324.56523	−327.46847
$HOCH_2NH_3^+$ **(13)**	−169.41035	−170.86377
$CH_2O \cdots H\text{-}NH_3^+$ **(14)**	−169.42186	−170.87301
NH_4^+ **(15)**	−56.18545	−56.68478
ts(11→16)	−324.55950	−327.45766
$(CH_3)_3COH \cdots CH_2NH_2^+$ **(16)**	−324.58804	−327.47911
$CH_2NH_2^+$ **(17)**	−93.80927	−94.63810
$(CH_3)_3COH$ **(18)**	−230.74028	−232.81268
$(CH_3)_2CCH_2 \cdots CH_2O$ **(19)**	−268.33943	−270.74623
$(CH_3)_3C^+$ **(20)**	−155.45763	−156.89435
$CH_2O \cdots NH_3$ **(21)**	−169.03903	−170.51059
CH_2OH^+ **(22)**	−113.47494	−114.42960
$(CH_3)_2CCH_2 \cdots NH_3^+$ **(23)**	−210.98178	−212.93839

resulting ion [1]. In the present case, however, the formaldehyde unit remains in place. This means that there must be a slight barrier for moving formaldehyde to the backside of the *i*-butene moiety, forming the proton bonded trimer (**7b**). The existence of this barrier is most likely related to the additional methyl group in the present case. No attempt to locate this transition state was made, and for simplicity only **7b** is shown in Fig. 3. Loss of formaldehyde gives $(CH_3)_2CCH_2 \cdots H\text{–}NH_3^+$ (**8**) as the resulting ion. The reaction enthalpy was calculated to be −35 kJ/mol.

In summary, the product ion with *m/z* 74 may either have the covalent structure or the complex structure depending on the mode of formation. In order to get some insight into this structural problem we isolated these product ions to investigate their further reactions with ammonia. A simplistic view would be that if the ions formed are $(CH_3)_3CNH_3^+$ then no further reactions with ammonia are expected. The proton bonded dimer could, however, be expected to react fast with ammonia in an exothermic ligand exchange reaction with the formation of a proton bonded ammonia dimer (**9**) (*m/z* 35) and *i*-butene (**10**). As indicated in Fig. 4 this reaction is exothermic by 63 kJ/mol. One single successful attempt to isolate *m/z* 74 was made, and no product ion with *m/z* 35 was observed in the reaction with ammonia. Therefore, the most likely interpretation is that the structure is $(CH_3)_3CNH_3^+$, since the back-side substitution mechanism was calculated to have the transition state that is lowest in energy.

3.2. The formation and reactions of $(C, H_6, N,O)^+$ ions (m/z 48.044)

There are two plausible structures of these ions; $HOCH_2NH_3^+$ (**13**) and $CH_2O \cdots H\text{–}NH_3^+$ (**14**), which both can be formed in exothermic reactions. The ab initio calculations show that the $HOCH_2NH_3^+$ ion may be formed in an addition-elimination (**ae**) type reaction where the ammonia molecule initially attacks the carbonyl carbon. The key step is then a proton transfer from the *t*-butyl part to oxygen, followed by elimination of *i*-butene. The transition structure [**ts(11→12)**] for this mechanism is, however, 15 kJ/mol higher in energy than the reactants—although it is exothermic by 30 kJ/mol. The formation of the proton bonded heterodimer between formaldehyde and ammonia (**14**) follows an elimination mechanism similar to the observed formation of $(CH_3)_2CCH_2 \cdots H\text{–}NH_3^+$ (**8**), except that *i*-butene (**10**) in this case is eliminated from the **7b**. The reaction exothermicity was calculated to be 54 kJ/mol.

Isolation of the *m/z* 48 ions and subsequent reaction with ammonia showed mainly formation of the proton bonded ammonia dimer (**9**), and in some cases a small amount of NH_4^+. Formation of $(NH_3)_2H^+$ (**9**) supports the idea that a major fraction of the *m/z* 48 ions formed are of the $CH_2O \cdots H\text{–}NH_3^+$ (**14**) type, because $HOCH_2NH_3^+$ (**13**) is not expected to react

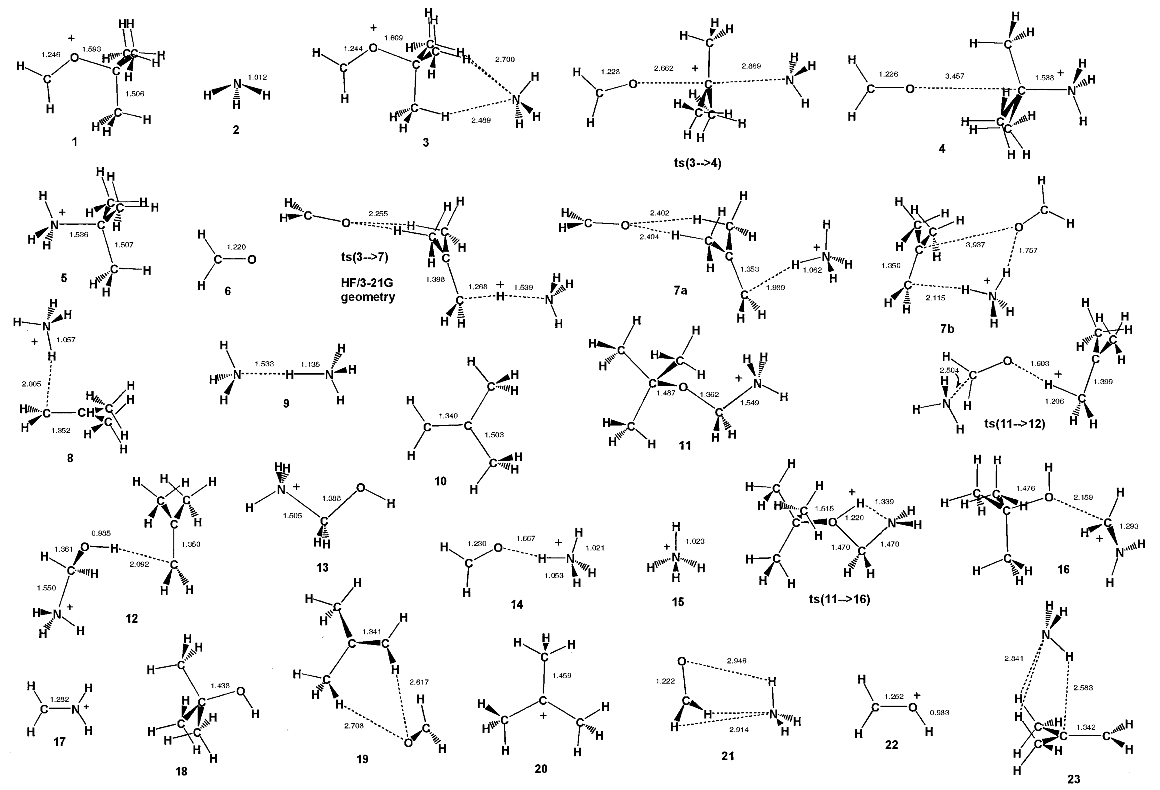

Fig. 3. Potential energy diagram from the MP2/6-31G(d,p) calculations. Relative energies are given in kJ/mol and include zpve corrections. See Table 1 for the actual values of the indicated energy parameters. The numbers indicated in the parenthesis are the numbers of the optimized structures shown in Fig. 2.

with ammonia in this way. This ligand exchange reaction is exothermic with 44 kJ/mol (Fig. 4). Due to the large dipole moment of formaldehyde, $CH_2O\cdots H{-}NH_3^+$ (**14**) is lower in energy than $(CH_3)_2CCH_2\cdots H{-}NH_3^+$ (**8**) despite that *i*-butene has higher proton affinity.

3.3. The formation and reactions of (N_2, H_7) ions (*m/z* 35.060)

As mentioned previously, the ion at *m/z* 35 is a proton bonded ammonia dimer (**9**) and it is a secondary reaction product. From the earlier discussion it seems reasonable that the main channel leading to this ion is an exothermic ligand exchange reaction between ammonia and $CH_2O\cdots H{-}NH_3^+$ (*m/z* 48). Isolation of *m/z* 35 shows no further reactions with ammonia, and this ion is in fact the dominant product at long reaction times together with NH_4^+.

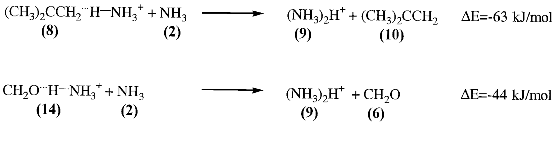

$$\underset{(8)}{(CH_3)_2CCH_2\cdots H{-}NH_3^+} + \underset{(2)}{NH_3} \longrightarrow \underset{(9)}{(NH_3)_2H^+} + \underset{(10)}{(CH_3)_2CCH_2} \quad \Delta E = -63\ \text{kJ/mol}$$

$$\underset{(14)}{CH_2O\cdots H{-}NH_3^+} + \underset{(2)}{NH_3} \longrightarrow \underset{(9)}{(NH_3)_2H^+} + \underset{(6)}{CH_2O} \quad \Delta E = -44\ \text{kJ/mol}$$

Fig. 4. Calculated reaction energies with MP2/6-31G(d,p) for the ligand exchange reactions.

3.4. The formation and reactions of (C,N,H_4) ions (*m/z* 30.033)

The signal at *m/z* 30 is from protonated methylene imine, $CH_2NH_2^+$ (**17**). It is formed in an addition-elimination (**ae**) reaction between $CH_2OC(CH_3)_3^+$ (**1**) and ammonia (**2**). The reaction is initiated by attack of ammonia at the carbonyl carbon, followed by a 1,3-proton transfer from nitrogen to oxygen (**ts(11 → 16)**) and subsequent elimination of *t*-butanol (**18**). The amount of *m/z* 30 was too small to allow for further isolation and subsequent reaction, but in a similar study [1] we have shown that when this ion reacts with ammonia, only slow thermoneutral [27] proton transfer is observed. As can be seen from the spectra of Fig. 1, the amount of the **ae** and **sub** products are of the same order of magnitude. A simplified theoretical comparison of these competing reactions was made by performing RRKM calculations (see Section 2). The only assumption, in addition to those already made by RRKM, was that both reactions occur through a common intermediate (**11**). This means that compared to the lifetime of the complexes **3** and **11**, the rearrangement between them is fast. Despite the quite significant differences in transition state energies, the calculations show that for ions with average thermal energy, the ratio k(**sub**)/k(**ae**) approaches 1.

3.5. The formation and reactions of NH_4^+ ions (m/z 18.034)

Proton transfer from $CH_2NH_2^+$ (**17**) to ammonia is thermoneutral [27]. The rather low rate coefficient, which we previously [1] measured to be $k = 1.9 \times 10^{-12}$ cm^{3}molecule^{-1}s^{-1}, is therefore surprisingly low—and from our kinetic modeling of the reaction it seems quite unlikely that $CH_2NH_2^+$ is the dominant source for NH_4^+. Since formation of NH_4^+ is fast (k is $\sim 10^{-10}$ cm^{3}molecule^{-1}s^{-1}) it is a good reason to conclude that the main source is $CH_2OC(CH_3)_3^+$ (**1**). There are, however, two problems with this argument. On one hand, the poor S/N ratio does not allow for a sufficiently precise kinetic modeling of the temporal variation in ion abundances. On the other hand, according to the MP2/6-31G(d,p) calculations the reaction

$$CH_2OC(CH_3)_3^+\ \mathbf{(1)} + NH_3\ \mathbf{(2)} \rightarrow NH_4^+\ \mathbf{(15)} + (CH_3)_2CCH_2\cdot\cdot\cdot CH_2O\ \mathbf{(19)} \qquad (3)$$

is endothermic by 17 kJ/mol. The latter statement is, however, uncertain. Only composite quantum chemical schemes like CBS-Q [28] and G2 [29] claim thermochemical accuracy better than 10 kJ/mol. This is evident when we compare the calculated difference in proton affinity between ammonia and *i*-butene with the experimental value (69.8 kJ/mol vs. 51.5 kJ/mol [27]). MP2/6-31G(d,p) overestimates this difference by 18.3 kJ/mol. At the same time, the MP2/6-31G(d,p) bond dissociation energy of **1** [to give $(CH_3)_3C^+$ and CH_2O] is 10 kJ/mol higher than the corresponding G2 value. In any instance the experimental evidence is clear in that proton transfer from **1** to ammonia is exothermic. We have considered the possibility that the remaining neutral product may have rearranged to a more stable isomer than $(CH_3)_2CCH_2\cdot\cdot\cdot CH_2O$ (**19**) during the process, thereby driving proton transfer to completion. Despite some effort we have not been able to find computational evidence for any hidden rearrangement.

The reason why the elimination reaction is dominating in this reacting system is probably that the transition state in this mechanism has a lot of low lying vibrational frequencies. RRKM reaction rate calculations using the HF/3-21G data show that k(**e**)/k(**sub**) $\approx$ 3 at the internal energy level of the reacting system. Wladkowski and Brauman [12] have observed that E2 dominates over S_N2 in the reaction between CN^- and $CH_3CHCl(CN)$, although S_N2 is the thermodynamically preferred reaction. Their belief is that the reason for this is a combination of a lower activation barrier and a looser transition state for the elimination pathway than for the substitution pathway. Gronert [14] has done theoretical calculations on the reactions between alkyl chlorides and F^- which show that elimination gets more favorable compared to substitution when the alkyl substitution on the α-carbon increases. He also predicts that E2 will dominate over S_N2 for *i*-propyl chloride. A combined experimental and theoretical study of the reactions between protonated alcohols and water by us [13] also show that elimination gets more favorable when the alkyl substitution on the α-carbon increases.

It turns out that the reactions can be explained from the attack of NH_3 (**2**) of either of the two electrophilic centers on $CH_2OC(CH_3)_3^+$ (**1**), as mentioned in the introduction. Attack at the carbonyl carbon leads to an **ae** reaction with the formation of the $CH_2NH_2^+$-ion (**17**). Attack at the substituent leads to either **sub** or **e** reactions with the formation of $(CH_3)_3CNH_3^+$ (**5**), $CH_2O\cdot\cdot H–NH_3^+$ (**14**) or NH_4^+(**15**). It is also evident that dimeric and trimeric ion-molecule complexes play a key role during the reaction.

A comparison for the CH_2OR^+/NH_3 reaction system ($R{=}C(CH_3)_3$) with the previously studied examples ($R{=}H$, CH_3, CH_2CH_3, $CH_2CH_2CH_3$, $CH(CH_3)_2$) [1], shows the expected trend in exothermisity and relative energy of the transition structures for the **sub** and **ae** reactions, except for the **sub** transition structure which is lower in energy than that for $R{=}CH(CH_3)_2$. This unexpected trend in reactivity for the *t*-butyl substituent has been observed by us in another S_N2-reaction [13]. In accordance with the previous paper [1] the relative energies of reactants, intermediates, transition structures, and products for the **ae** and **sub** reaction all give good linear relationships when plotted against the alkyl cation stabilization constants. The rate constant for disappearance of the ionic reactant in the case of $R{=}C(CH_3)_3$ was estimated to be $\sim 5 \times 10^{-10}$ $cm^3 molecule^{-1} s^{-1}$, which is about the same as for $R{=}H$, CH_3, CH_2CH_3, $CH_2CH_2CH_3$, and $CH(CH_3)_2$. However, in the latter five cases only **ae** and **sub** reactions were observed, whereas in the former the **e** reaction is dominating. The signal-to-noise ratio in the present experiments is too low to obtain sufficiently precise rate constants for the **ae** and **sub** reactions. A rough estimate is that both are around 10^{-12} $cm^3 molecule^{-1} s^{-1}$.

4. Conclusion

The two major reaction paths for the direct reactions between the *t*-butyl methylene oxonium ion and ammonia are proton transfer to ammonia and formation of the proton bonded formaldehyde-ammonia heterodimer. The dimeric species reacts fast with ammonia in a ligand exchange reaction resulting in formation of a proton bonded ammonia dimer. Two minor reaction channels are also observed, a nucleophilic substitution reaction which leads to the formation of protonated *t*-butylamine and formaldehyde, and an addition-elimination reaction where the products are protonated methylene imine and *t*-butanol.

Acknowledgements

The authors wish to thank Mr. Vidar Bjørnstad, University of Oslo, for the synthesis of *t*-butyl *n*-propyl ether, and NFR (the Norwegian Research Council) for computer time.

References

[1] L. Bache-Andreassen, E. Uggerud, Int. J. Mass Spectrom. 195/196 (2000) 171.
[2] M.C. Caserio, J.K. Kim, J. Org. Chem. 47 (1982) 2940.
[3] S. Okada, Y. Abe, S. Taniguchi, S. Yamabe, J. Am. Chem. Soc. 109 (1987) 295.
[4] R. van Doorn, N.M.M. Nibbering, Org. Mass Spectrom. 13 (1978) 527.
[5] H.E. Audier, T.B. McMahon, J. Mass Spectrom. 32 (1997) 201.
[6] G. van der Rest, G. Bouchoux, H.E. Audier, T.B. McMahon, Eur. Mass Spectrom. 4 (1998) 339.
[7] M. Pykäläinen, A. Vainiotalo, T. Pakkanen, P. Vainiotalo, J. Mass Spectrom. 31 (1996) 716.
[8] M.A. Freitas, R.A.J. O'Hair, Int. J. Mass Spectrom. Ion Processes 175 (1998) 107.
[9] J.K. Pau, J.K. Kim, M.C. Caserio, J. Am. Chem. Soc. 100 (1978) 3838.
[10] P.F. Wilson, M.J. McEwan, M. Meot-Ner, Int. J. Mass Spectrom. Ion Processes 132 (1994) 149.
[11] C.H. DePuy, S. Gronert, A. Mullin, V.M. Bierbaum, J. Am. Chem. Soc. 112 (1990) 8650.
[12] B.D. Wladkowski, J.I. Brauman, J. Am. Chem. Soc. 114 (1992) 10643.
[13] E. Uggerud, L. Bache-Andreassen, Chem. Eur. J. 5 (1999) 1917.
[14] S. Gronert, J. Am. Chem. Soc. 115 (1993) 652.
[15] H.E. Audier, D. Berthomieu, J. Org. Chem. 60 (1995) 7198.
[16] D. Berthomieu, H.E. Audier, Eur. Mass Spectrom. 3 (1997) 19.
[17] K. Norrman, T.B. McMahon, J. Am. Chem. Soc. 118 (1996) 2449.
[18] L.J. de Konig, N.M.M. Nibbering, S.L. van Orden, F.H. Laukien, Int. J. Mass Spectrom. Ion Processes 165/166 (1997) 209.
[19] J.F. Norris, G.W. Rigby, J. Am. Chem. Soc. 54 (1932) 2088.
[20] M.J. Frisch, G.W. Trucks, H.B. Schlegel, P.M.W. Gill, B.G. Johnson, M.A. Robb, J.R. Cheeseman, T.A. Keith, G.A. Peterson, J.A. Mongomery, K. Raghavachari, M.A. Al-Laham, V.G. Zakrzewski, J.V. Ortiz, J.B. Foresman, J. Cioslowski, B.B. Stefanov, A. Nanayakkara, M. Challacombe, C.Y. Peng, P.Y. Ayala, W. Chen, M.W. Wong, J.L. Andres, E.S. Reploge, R. Gomperts, R.L. Martin, D.J. Fox, J.S. Binkley, D.J. Defrees, J. Baker, J.J.P. Stewart, M. Head-Gordon, C. Gonzalez, J.A. Pople, GAUSSIAN94, Gaussian Inc., Pittsburg, Pennsylvania, 1994.

[21] M.J. Frisch, G.W. Trucks, H.B. Schlegel, G.E. Scuseria, M.A. Robb, J.R. Cheeseman, V.G. Zakrzewski, J.A. Mongomery, R.E. Stratmann, J.C. Burant, S. Dapprich, J.M. Millam, A.D. Daniels, K.N. Kudin, M.C. Strain, O. Farkas, J. Tomasi, V. Barone, M. Cossi, R. Cammi, B. Mennucchi, C. Pomelli, C. Adamo, S. Clifford, J. Ochterski, G.A. Peterson, P.Y. Ayala, Q. Cui, K. Morokuma, D.K. Malick, A.D. Rabuck, K. Raghavachari, J.B. Forsman, J. Cioslowski, J.V.B. Ortiz, A.G., B.B. Stefanov, G. Liu, A. Liashenko, P. piskorz, I. Komaromi, R. Gomperts, R.L. Martin, D.J. Fox, T. Keith, M. Al-Laham, C.Y. Peng, A. Nanayakkara, C. Gonzales, M. Challacombe, P.M.W. Gill, B.G. Johnson, W. Chen, M.W. Wong, J.L. Andres, A. Gonzales, M. Head-Gordon, E.S. Reploge, J.A. Pople, GAUSSIAN 98, Gaussian Inc., Pittsburg, Pennsylvania, 1998.

[22] C.C.J. Roothan, Rev. Mod. Phys. 23 (1951) 69.

[23] C. Møller, M.S. Plesset, Phys. Rev. 46 (1934) 618.

[24] M.J. Frisch, J.A. Pople, J.S. Binkley, J. Chem. Phys. 80 (1984) 3265.

[25] A.P. Scott, L. Radom, J. Phys. Chem. 100 (1996) 16502.

[26] R.G. Gilbert, S.C. Smith, Theory of Unimolecular and Recombination Reactions, Blackwell Scientific, Oxford, 1990.

[27] NIST Chemistry WebBook, NIST Standard Reference Database Number 69, W.G.M.a.P.J. Linstrom (Ed.), 2000, National Institute of Standards and Technology, Gaithersburg MD, 20899 (http://webbook.nist.gov).

[28] G.A. Petersson, T.G. Tensfeldt, J.A. Montgomery, Jr., J. Chem. Phys. 94 (1991) 6091.

[29] L.A. Curtiss, K. Raghavachari, G.W. Trucks, J.A. Pople, J. Chem. Phys. 94 (1991) 7221.